ISSN 1061-933X, Colloid Journal, 2024, Vol. 86, No. 2, pp. 169–177. © Pleiades Publishing, Ltd., 2024.

Refraction of Hydrosols Containing Diamond/Amorphous Carbon Composite Particles

O. S. Vezo[a], A. V. Voitylov[a], V. V. Vojtylov[a], M. P. Petrov[a, *], and A. A. Trusov[a]

[a] *Department of Physics, St. Petersburg State University, Petrodvorets, St. Petersburg, 198504 Russia*

**e-mail: m.p.petrov@spbu.ru*

Received December 8, 2023; revised December 29, 2023; accepted December 29, 2023

Abstract—Refractometric studies of hydrosols containing diamond nanoparticles have been carried out in this work. The samples for the study have been obtained from a statically synthesized diamond powder preliminarily subjected to standard purification by washing with strong acids and sonication. After additional repeated washing, centrifugation, sonication, and settling for a month, samples, whose particles contained different fractions of amorphous carbon, have been obtained. The particle size in the obtained samples was smaller than 100 nm. To analyze the data of refractometric measurements, equations have been derived that make it possible to determine the fraction of amorphous carbon in the particles and to calculate the thickness of its layer on the particle surface from the results of studying the refractive index and density of the sols of diamond particles. The data of the refractometric studies have been used to determine the ratios between the fractions of crystalline diamond and amorphous carbon in the particles. The performed studies have shown that the refractometric analysis of particle composition can be used to control the quality of industrially produced nanodiamonds.

Keywords: nanodiamond, amorphous carbon, refraction, light scattering, electrooptical method, X-ray diffraction analysis

DOI: 10.1134/S1061933X24600040

INTRODUCTION

Optical methods are powerful tools that enable one to implement a nondestructive analysis of colloids and suspensions and control their stability.

Diamond sols obtained by various methods have pronounced optical properties. Such properties include luminescence [1], absorption and scattering of light [2–5], and electrooptical effect [6–8]. High-intensity luminescence is generated by defects located inside and on the surface of diamond particles [9–12]. The high coagulation stability of diamond hydrosols and the inertness of the particles have opened broad prospects of using thereof as labels for biosystems in medicine instead of semiconductor quantum dots, which are highly toxic [13, 14]. The study of the optical density of nanodiamond sols has made it possible to confirm the hypothesis about the existence of the Pandey chains on the particle surface [15]. It has also been noted that different modifications of carbon may be present on diamond particle surfaces, with these modifications containing π electrons that may be displaced along a surface similarly to free electrons in metals [16]. Important problems are the production of stable nanodiamond sols and the study of the formation kinetics of particle aggregates. Static and dynamic light scattering methods are employed to analyze the sizes and shapes of particles and determine their coagulation thresholds [17]. Electrooptical methods enable one to determine the particle size distribution functions and the polarizability values in polydisperse systems, as well as to study the coagulation kinetics of diamond sols at the stage of aggregate formation from a small number of particles [18]. They have also been used to study the polarizability and surface conductivity of diamond particles in aqueous electrolytes [19].

Composite materials containing diamond and amorphous carbon are of wide scientific interest [20, 21]. Such composites are used in the production of films. The structural shells of noncrystalline carbon on the surface of diamond particles determine, in many respects, the properties of the particles themselves and the materials containing such particles [22, 23]. The studies have shown that functional groups predetermine the optical properties of both nano- and microdiamonds, as well as their disperse systems [24]. While intense light scattering by particles in liquid disperse systems containing microparticles determines their basic optical properties, in the case of liquid disperse systems of nanoparticles exhibiting weak light scattering, refractometric studies may provide important information about both the internal and surface composition of the particles. The results of studying the refractive indices of hydrosols containing nano-

sized particles composed of crystalline diamond and amorphous carbon have been presented and analyzed in this work.

THEORETICAL

If particles of a disperse system are small as compared with the light wavelength (Rayleigh particles), they scatter light as dipoles subjected to a uniform electric field of the light wave. If the particle concentration is sufficiently high, a sphere, whose diameter does not exceed the light wavelength, contains a large number of particles, their electric dipole moments induced by the light wave are enhanced by the fields of other particles, and the light refraction in such disperse system is similar to the refraction of a molecular solution [25]. This approach was previously considered when studying carbon black to determine the refractive index of graphite [26]. At low concentrations of particles in a disperse system, they scatter light as individual particles.

The refractive indices of such disperse systems should be considered to be complex, even when the particles and the dispersion medium do not absorb light, because a light beam passing through such a disperse system loses its intensity due to light scattering by the particles. When describing the light refraction in disperse systems, one may use the scattering amplitude function, which is determined as the sum of the scattering amplitude functions of the particles. Assuming the amplitude of an incident wave to be equal to unity, the $S_j(\vartheta, \varphi)$ scattering amplitude function for an individual spherical particle is determined by the following equation [27]:

$$u = S_j(\vartheta, \varphi)\frac{e^{-ikr+i\omega t}}{ikr},$$

where u is a scattered wave at a large distance from the particle, k is the wave vector, r is the distance from the particle, and ω is the frequency of the incident light wave. When describing refraction, it is necessary to consider the forward scattering, which corresponds to $\vartheta = 0$ and $\varphi = 0$.

At a low particle concentration, refractive indices of a disperse system m_s and a dispersion medium m_0 are close, and it may be stated that [27]

$$m_s - m_0 = -i2\pi k'^{-3} S(0), \quad (1)$$

where $S(0) = \sum_{j=1}^{N} S_j(0)$, $k' = 2\pi|m_0|/\lambda$, λ is the light wavelength in vacuum, and N is the number of particles per unit volume.

For monodisperse systems of small particles, which are polarized in the field of a light wave as individual particles, the $S(0)$ amplitude function for a disperse system can be represented by the following relation [27]

$$S(0) = \alpha N\left(ik'^3 + \frac{2}{3}k'^6\alpha\right). \quad (2)$$

Particle polarizability α, which enters into Eq. (2), may be determined by relation [28]

$$\alpha = \frac{3V}{4\pi}\frac{m_p^2 - m_0^2}{m_p^2 + 2m_0^2}, \quad (3)$$

in which V is the particle volume and m_p is the particle refractive index. If particles absorb light, m_p is a complex value.

Taking into account Eq. (3), αN can be represented by relation

$$\alpha N = \frac{3\theta}{4\pi}\frac{m_p^2 - m_0^2}{m_p^2 + 2m_0^2}, \quad (4)$$

in which $\theta = VN$ is the volume fraction of particles in the disperse system.

Substituting Eqs. (2)–(4) into Eq. (1), we arrive at the following relation:

$$m_s - m_0 = \frac{3\theta}{2}\left(\frac{m_p^2 - m_0^2}{m_p^2 + 2m_0^2} - i\frac{k'^3 V}{2\pi}\left(\frac{m_p^2 - m_0^2}{m_p^2 + 2m_0^2}\right)^2\right). \quad (5)$$

If $V \ll \lambda^3$, the second term in the parentheses is small and can be ignored. The volume fraction of the particles can be determined, provided that the densities of the dispersion medium ρ_0, disperse system ρ_s, and particles ρ_p are known. The value of θ can be represented as

$$\theta = \frac{\rho_s - \rho_0}{\rho_p - \rho_0}, \quad (6)$$

and, taking into account Eq. (5), increment M of the refractive index can be determined by relation

$$M = \frac{m_s - m_0}{\rho_s - \rho_0} = \frac{3}{2(\rho_p - \rho_0)}\frac{m_p^2 - m_0^2}{m_p^2 + 2m_0^2}. \quad (7)$$

The right-hand side of Eq. (7) is independent of m_s and ρ_s. The plot of the m_s–ρ_s dependence is a straight line, the slope of which is represented by the right-hand side of relation (7). The left-hand side of Eq. (7) can be determined experimentally by varying the particle concentration in a studied disperse system and experimentally determining the resulting changes in m_s and ρ_s. If the values of ρ_p, ρ_0, and m_0 are known, m_p can be found as a solution of Eq. (7). Relation (7) does not comprise particle sizes, and it is applicable to polydisperse systems, provided that the particles are small.

If the particles are commensurable with the light wavelength, their contribution to the refractive index of the disperse system decreases significantly with an increase in the particle sizes. In the case of a mono-

disperse system containing spherical particles, general relation (1) can be transformed into the form of

$$m_s - m_0 = -i\frac{3S_p(0)\theta}{2(k'r)^3}. \quad (8)$$

Here, r is the radius of the particles and $S_p(0)$ is their amplitude function.

The $S_p(0)$ function can be found using the Mie theory, [29, chapters VI, VII]. Having determined the dependence of $m_s - m_0$ on particle sizes, it becomes possible to estimate the range of their variations to which relation (7) is applicable. According to the Mie theory, numerical methods were employed to calculate the real components of particle refractive indices n_s using Eq. (8) for the longest wavelength (λ = 657.2 nm) of the refractometer that we used. Dependences of difference $n_s - n_0 = \mathrm{Re}(m_s - m_0)$ on size r for aqueous disperse systems containing diamond and graphite particles are presented in Fig. 1. The calculations were performed under the assumption that volume fraction θ remained unchanged.

Figure 1 shows that, at $r < 100$ nm, changes in particle sizes have a weak effect on the $(n_s - n_0)/(\rho_s - \rho_0)$ ratio. In this range of particle sizes, relation (7) can be used at wavelengths of 657.2 nm and above. However, as follows from Fig. 1, an increase in size r within a range of 100–200 nm leads to a significant decrease in $(n_s - n_0)/(\rho_s - \rho_0)$. It can be seen in Fig. 1 that, at $r > 200$ nm, the $(n_s - n_0)/(\rho_s - \rho_0)$ ratio is negligible for disperse systems with diamond particles; moreover, in the case of graphite particles, it decreases by more than two times.

The imaginary component of refractive index m_s can be determined by nephelometry. However, when studying polydisperse systems using this method, it is necessary to take into account the particle size distribution, even if the particles are small. This is due to the fact that the light energy scattered by particles, which determines the intensity of the beam passing through the disperse system, significantly depends on the particle sizes. This paper presents the results of studying the real component of m_s.

EXPERIMENTAL

The following parameters were determined in the experiments: the refractive indices of aqueous disperse systems of diamond, the volume fraction of particles in them, the relaxation curves of the electrooptical effect observed in the disperse systems, electron microscopic images of particles, and the X-ray diffraction spectra of the dispersed phase.

The volume fraction of the particles was determined using relation (6). The densities of disperse systems and dispersion media contained in this ratio were determined with an accuracy of 5×10^{-6} g/cm^3 using a DMA 5000M densitometer.

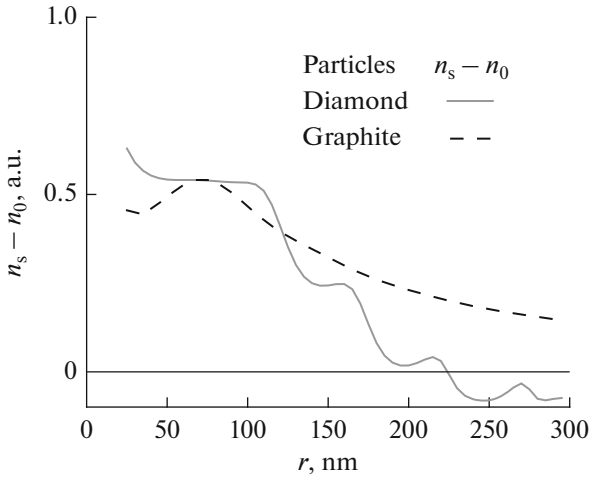

Fig. 1. Dependence of $(n_s - n_0)/(\rho_s - \rho_0)$ on r at λ = 657.2 nm.

The absolute values of the refractive indices of the studied disperse systems and dispersion media were determined using an Abbemat WR/MW refractometer. The measurement accuracy of the refractive index of a disperse system was 4×10^{-5} nD. Relative measurements were performed using the Rayleigh method. The measurements were carried out using an ITR-2 interference-type refractometer. The accuracy of such measurements was no worse than 1×10^{-6} nD.

Average size r of nanodiamond particles was determined by the standard dynamic light scattering (DLS) method. The experimental studies were implemented with a serial Photocor Complex device.

The electrooptical (EO) method was used to determine the size distribution functions of nanodiamond particles and their aggregates in a size range above 25 nm. The accuracy of its determination by the EO method was better than that by the DLS method; however, the EO method is inapplicable to disperse systems that are destroyed when being exposed to pulsed electric fields that cause orientational ordering of particles. The disperse systems studied in this work did not have high electrical conductivity and were resistant to the action of electric fields imposed on them. Electrical dichroism (ED) is highly pronounced in diamond and graphite sols. Namely, when particles are oriented in an electric field, a difference characteristic of dichroism arises in the optical density values for light beams polarized in parallel and perpendicularly to the electric field, which causes the orientational ordering of the particles. ED can be defined as the difference between the relative changes induced in the optical density by the electric field for these beams. The relaxation dependence of the ED is related to the

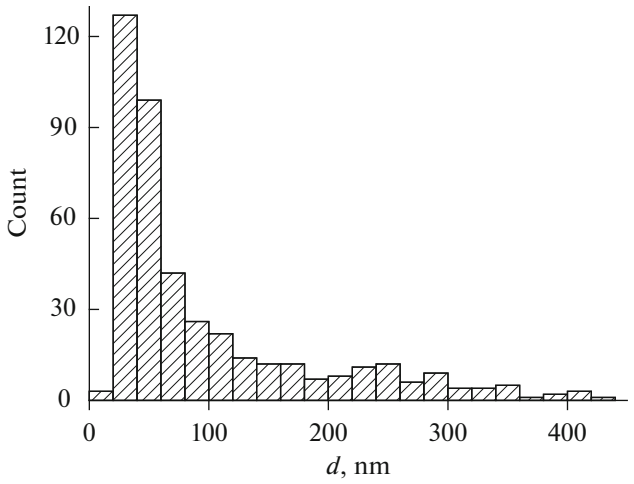

Fig. 2. Size distribution of diamond particles.

particle size distribution function by the following expression [18]:

$$N(t) = \int \exp(-6D_r t)\Delta K(r)\varphi(r)dr. \quad (9)$$

Here, $N(t)$ is the relaxation dependence of the ED, $\varphi(r)$ is the particle size distribution function, D_r is the rotational diffusion coefficient of particles and their aggregates (it varies in inverse proportion to r^3). If white light is used to determine $N(t)$, $\Delta K(r) = Cr^2$, where C is the normalization coefficient [30]. Having determined the $N(t)$ dependence experimentally, $\varphi(r)$ can be calculated by solving integral equation (9). In this article, $N(t)$ was determined using the experimental setup designed by the authors of [19], while the $\varphi(r)$ function was found by the regularization method [8].

X-ray diffraction analysis of the particles was carried out with an R-axis Rigaku diffractometer (CoK_α radiation, $\lambda = 1.789$ Å), while a Zeiss Supra 40VP scanning microscope was used to obtain electron microscopic images.

DISPERSE SYSTEMS UNDER INVESTIGATION

Samples to be studied were obtained using a commercial powder containing nanodiamond particles produced by static synthesis. This powder had been subjected to preliminary purification. For the research, an additional purification was required. According to the published data, after purification with acids and mechanical cleaning, the particles resulting from the synthesis had an internal crystalline structure of diamond covered with a shell formed from carbon of other forms [31]. After the additional purification, including washing in distilled water and repeated alternating sonication and centrifugation, a dispersed phase was obtained that did not contain large particles and their aggregates. A histogram of the distribution of dispersed phase diamond particles over size d is presented in Fig. 2 (d is the average size in the image). This histogram was obtained using the results of processing electron microscopic images of the particles.

In order to determine the allotropic forms of carbon other than crystalline diamond in the dispersed phase, an X-ray diffraction analysis was carried out, which showed that the diamond dispersed phase had a polycrystalline structure inherent in aggregates of small particles containing additives of amorphous carbon. Then, during the sedimentation for a month, the dispersed phase suspended in water was fractionated into layers, which had a uniform composition and different colors and were separated by distinct boundaries. Four samples resulting from sedimentation of the initial disperse system were selected for the studies. The tint varied from dark gray for the top layer (sample 1) to light gray for the bottom layer (sample 4). The obtained samples were used to prepare hydrosols with a particle content of less than 0.01 wt %. Shaking and sonication made it possible to maintain unchanged optical properties of the sols for a long time that was necessary for the investigations.

Previous studies of light scattering by diamond sols [32] had led to the conclusion that the light scattering by diamond particles is typical for spherical ones, in spite of their irregular shapes. Hence, when studying aqueous disperse systems of diamond, we may use Eqs. (7) and (8), which were obtained under the assumption that the particles were polarized in the field of a light wave as spherical ones.

RESULTS AND DISCUSSION

For all isolated fractions, the $\varphi(r)$ particle size distribution functions were determined using the electrooptical method. Samples 1–4 contained particles and aggregates with differed sizes. The $\varphi(r)$ functions of these samples are shown in Fig. 3.

The control measurements performed by the DLS method corresponded to the results presented in Fig. 3. The diffraction patterns obtained by the X-ray diffraction analysis (CoK_α radiation, $\lambda = 1.789$ Å) of the dispersed phases of these samples are presented in Fig. 4.

As is seen in Fig. 4, in the diffraction angle regions of 51.3°, 90.3°, and 112.3°, peaks characteristic of diamond are observed for all samples. In an angle region of 30.5°, peaks characteristic of graphite 2H (30.5°) and 3R (31.0°) are seen for all samples. A wide band with a maximum at 20° corresponds to amorphous carbon. Peaks characteristic of a graphite-like structure and amorphous carbon indicate that a part of carbon in the particles of all samples is in a state other than the diamond crystal lattice. In this case, the content of amorphous carbon cannot be assessed quantitatively. However, it can be stated that, for the first

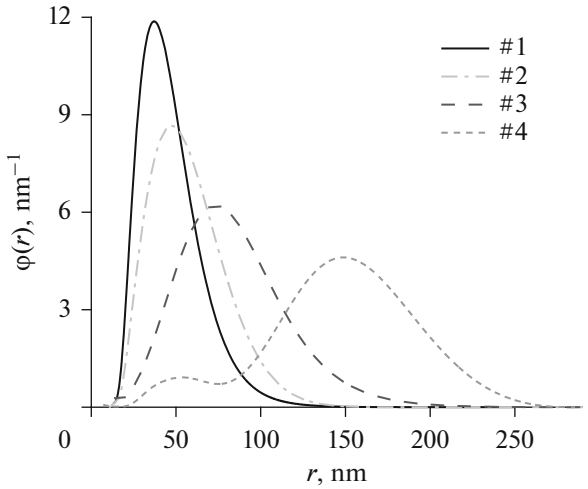

Fig. 3. Particle size distribution functions.

sample, the fraction of amorphous carbon in the particles is larger than that for the others.

Volume fraction θ of particles in the studied samples was varied by diluting them with distilled water. The particle volume fraction maximum permissible for measuring the refractive indices of the samples depended on their turbidity and did not exceed 3×10^{-4}. By diluting the samples with distilled water, disperse systems were obtained, for which densities ρ_s and refractive indices $n_s = \mathrm{Re}(m_s)$ were determined experimentally. For sample 4, the particle sizes of which are close to the light wavelength, no effect of particles on the refractive index was detected. This was due to the extremely small difference between the refractive index of the disperse systems obtained from this sample and the refractive index of water, even at volume fraction $\theta = 0.33 \times 10^{-4}$ of particles maximum permissible for this sample with respect to turbidity. For disperse systems containing particles of other samples, the dependences of n_s on ρ_s were linear. The dependence of n_s on ρ_s determined for sample 2 is presented in Fig. 5.

In addition, Fig. 5 presents variations in the real component of the refractive index theoretically calculated by Eq. (7) for disperse systems containing amorphous carbon particles and diamond particles, for which refractive index increment $(n_s - n_0)/(\rho_s - \rho_0)$ was equal to 0.87 and 0.26 cm^3/g, respectively.

For samples 1–3, the $(n_s - n_0)/(\rho_s - \rho_0)$ values obtained at $\lambda = 657.2$ nm are presented in Table 1. The error in the presented values was 2%.

Here it should be taken into account that, if a particle has a surface layer, its influence on the particle polarization in an electric field is significantly higher than the influence of the internal part of the particle. In the case of small colloidal particles, even a monomolecular layer containing adsorbed molecules of surfactants and having additional chemical bonds can significantly affect the polarizability of the particles in a

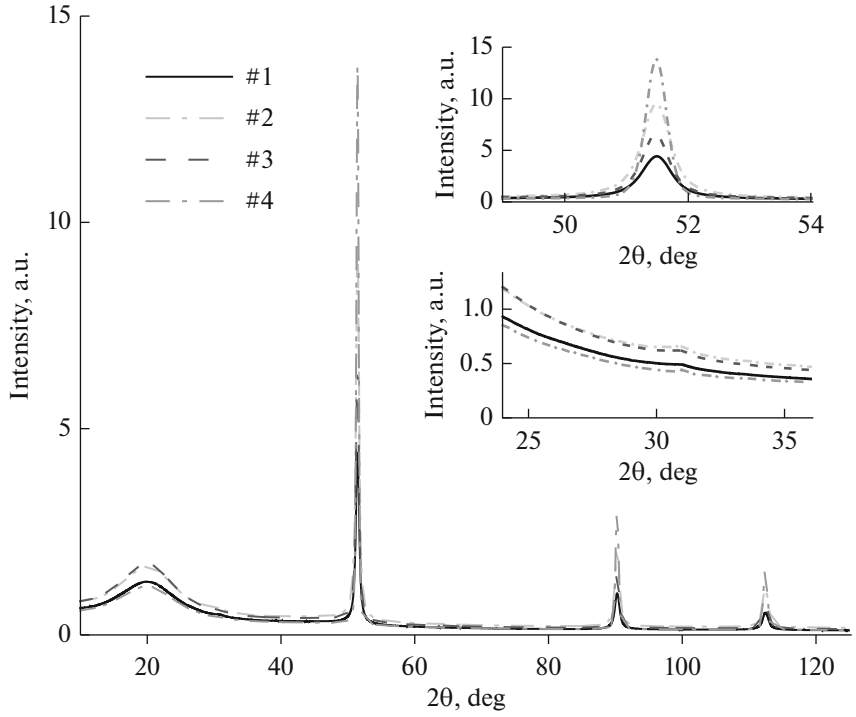

Fig. 4. Diffraction pattern of dispersed phase.

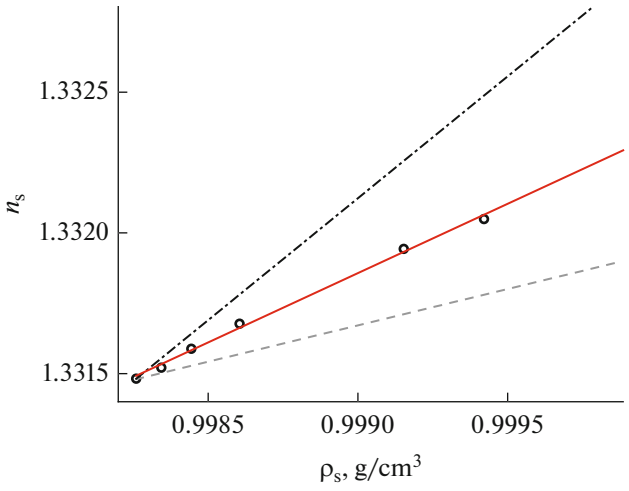

Fig. 5. Dependences of n_s on ρ_s at $\lambda = 657.2$ nm. Dots refer to experimental data; dashed and dash-and-dot lines denote diamond and amorphous carbon particles, respectively.

dispersion medium, and, hence, the difference in refractive indices $m_s - m_0$. Such a particle can be considered as multilayer, and refractive index m_p present in relation (7) must take into account the optical properties of the surface layer of the particles.

As follows from the theory, the main contribution to the polarization of a two-layer sphere is made by the polarization of the external layer, while the polarization of the internal part of the sphere is only a small additive to its total polarization [27, 33]. Equation (3), which enables one to determine the polarizability of a particle, is applicable under the condition that the particle size is small as compared with the light wavelength, both outside and inside of the particle, namely: $2\pi \mid m_0 \mid r \ll \lambda$ and $2\pi \mid m_p \mid r \ll \lambda$. If a particle or its surface layer has a high electric conductivity, the electric field of the light wave does not penetrate the particle, and the second inequality is reversed [27]. It should be noted that, for diamond and amorphous carbon, the values $\mathrm{Re}\,(m^2)$ are close, and the polarization of a diamond particle coated with a layer of amorphous carbon weakly depends on the thickness of the layer. Absorption $\mathrm{Im}\,(m^2)$ of light energy by the external layer only weakens the influence of the polarizability of the internal part of the particle on its total polarizability.

Table 1. Experimentally determined values of $(n_s - n_0)/(\rho_s - \rho_0)$

Sample	1	2	3
$(n_s - n_0)/(\rho_s - \rho_0)$	0.49	0.44	0.43

For uniform diamond particles, it should be assumed that $m_p = n_p = 2.42$; if the particles are covered with a layer of amorphous carbon, $m_p = 2.70 - i1.29$, while, for particles with an electrically conductive surface $\mid m_p \mid \approx \infty$.

The density of a particle with a surface layer (a two-layer sphere) depends significantly on the layer thickness, because the densities of diamond and amorphous carbon differ significantly.

Values $M = (m_s - m_0)/(\rho_s - \rho_0)$ were calculated for aqueous disperse systems containing particles corresponding to all three considered cases. It was assumed that the surface layer was thin and the particle density was equal to the density of diamond, $\rho_p = 3.5$ g/cm^3. The results of calculating M by Eq. (7) are presented in Table 2.

An increase in surface layer thickness h weakly affects the refractive index of particles; however, its effect on particle density ρ_p must be taken into account, since the densities of diamond and amorphous carbon differ significantly. Taking into account the densities of diamond ρ_D and amorphous carbon ρ_C, as well as volume fraction β of the surface layer in the particle, its density ρ_p can be represented by relation

$$\rho_p = (1 - \beta)\rho_D + \beta\rho_C. \qquad (10)$$

Substituting the value of ρ_p from relation (10) into relation (7) and taking into account that $\mathrm{Re}(M) = (n_s - n_0)/(\rho_s - \rho_0)$, volume fraction β may be represented as

$$\beta = \frac{\rho_D - \rho_0}{\rho_D - \rho_C} - \frac{3}{2(\rho_D - \rho_C)} \times \left(\frac{n_s - n_0}{\rho_s - \rho_0}\right)^{-1} \mathrm{Re}\left(\frac{m_p^2 - m_0^2}{m_p^2 + 2m_0^2}\right). \qquad (11)$$

Ratio h/r for a spherical particle

$$\frac{h}{r} = 1 - \sqrt[3]{1 - \beta} \qquad (12)$$

enables one to determine thickness h of the surface layer for particles with a given size.

For samples 1–3, the values of β and h/r are presented in Table 3. In calculations performed by Eqs. (11) and (12), it was assumed that $m_p = 2.70 - i1.29$, and the density of the amorphous carbon layer is $\rho_C = 2.15 \pm 0.08$ g/cm^3 [34]. The $(n_s - n_0)/(\rho_s - \rho_0)$ values required for the calculation of β for these samples are presented in Table 1. The most probable values of r for particles in samples 1–3 were used to determine thickness h of the surface layer of the particles. The values of h are also presented in Table 3. Taking into account the inaccuracy in the determination of ρ_C, the error in the determination of β was 8%.

Table 2. Values of M calculated for different polarizations of the surface layer of diamond particles in aqueous sols

Surface layer of particles	None	Amorphous carbon	Electrically conductive layer
m_p	2.42	$2.70 - i1.29$	∞
M, cm^3/g	0.26	$0.38 - i0.17$	0.60

Table 3. Volume fraction and thickness of amorphous carbon layer in the particles

Sample	1	2	3
β Refraction method	0.40–0.45	0.25–0.27	0.21–0.24
h/r	0.16	0.06	0.08
h, nm	4.8	3.9	6.8

CONCLUSIONS

The performed studies have shown that the refractometric method is applicable to the study of disperse systems, the particles of which are small as compared with the light wavelength. In combination with the electrooptical method or the dynamic light scattering method, the refractometric method can be used to study the properties of the surface layer of particles and the structure of their aggregates. The study of aqueous disperse systems of diamond has resulted in determining the fraction of amorphous carbon in the particles and the thickness of the layer, which it forms.

The procedure considered in this work enables one to perform the rapid analysis of the quality of purification of industrially produced nanodiamonds for particles that are small as compared with the light wavelength. The procedure involves the measurement of only the density and refractive index of colloidal diamond solutions, which can be performed quickly and accurately.

ACKNOWLEDGMENTS

The analysis of particles and their surfaces was supported by the Resource Centres of the Research Park of St. Petersburg State University: Interdisciplinary Resource Centre for Nanotechnology; the Centre for Optical and Laser Materials Research; the Centre for Diagnostics of Functional Materials for Medicine, Pharmacology and Nanoelectronics; the Centre for Physical Methods of Surface Investigation; and the Centre for X-ray Diffraction Studies. The authors are grateful to the staff of the centres for their support.

FUNDING

This work was supported by ongoing institutional funding. No additional grants to carry out or direct this particular research were obtained.

CONFLICT OF INTEREST

The authors of this work declare that they have no conflicts of interest.

REFERENCES

1. Mikheev, K.G., Shenderova, O.A., Kogai, V.Y., Mogileva, T.N., and Mikheev, G.M., Raman spectra of nanodiamonds of detonation and high-pressure high-temperature synthesis and the effect of laser action on their luminescence spectra, *Khim. Fiz. Mezoskopiya*, 2017, vol. 19, no. 3, pp. 396–406.
2. Reich, K.V., Optical properties of nanodiamond suspensions, *JETP Lett.*, 2011, vol. 94, no. 1, pp. 22–26. https://doi.org/10.1134/S0021364011130169
3. Mikheev, G.M., Vanyukov, V.V., Mogileva, T.N., Puzyr', A.P., Bondar', V.S., and Svirko, Y.P., Saturable absorption in aqueous suspensions of detonation nanodiamonds under irradiation with femtosecond laser pulses, *Tech. Phys. Lett.*, 2015, vol. 41, no. 12, pp. 1163–1166. https://doi.org/10.1134/S1063785015120263
4. Grinyaev, N.S., Nyavro, A.V., Koptsev, A.P., and Cherepanov, V.N., Broadband absorption of diamond nanoclusters, *Izv. Vyssh. Uchebn. Zaved., Fiz.*, 2012, vol. 55, no. 8/2, pp. 173–174.
5. Mikheev, G.M., Vanyukov, V.V., Mogileva, T.N., Mikheev, K.G., Aleksandrovich, A.N., Nunn, N.A., and Shenderova, O.A., Femtosecond optical nonlinearity of nanodiamond suspensions, *Applied Sciences*, 2021, vol. 11, no. 12, p. 5455. https://doi.org/10.3390/app11125455
6. Klemeshev, S.A., Petrov, M.P., Trusov, A.A., and Vojtylov, V.V., Light scattering in colloids of diamond and graphite, *Colloids Surf., A*, 2012, vol. 400, pp. 52–57. https://doi.org/10.1016/j.colsurfa.2012.02.045
7. Petrov, M.P., Voitylov, V.V., Klemeshev, S.A., and Trusov, A.A., Effect of electric field on light scattering by aqueous colloids of diamond and graphite, *Opt. Spectrosc.*, 2011, vol. 111, no. 5, pp. 832–840. https://doi.org/10.1134/S0030400X11090207
8. Babadzhanyants, L.K., Voitylov, A.V., Voitylov, V.V., and Trusov, A.A., Analysis of polydispersity of macromolecular and nanodisperse systems by electrooptical methods, *Polymer Science Series C*, 2010, vol. 52, pp. 93–104. https://doi.org/10.1134/S181123821001011X
9. Vlasov, I.I., Shenderova, O., Turner, S., Lebedev, O.I., Basov, A.A., Sildos, I., Rähn, M., Shiryaev, A.A., and Van Tendeloo, G., Nitrogen and luminescent nitrogen-vacancy defects in detonation nanodiamond, *Small*, 2010, vol. 6, no. 5, pp. 687–694. https://doi.org/10.1002/smll.200901587

10. Baranov, P.G., Soltamova, A.A., Tolmachev, D.O., Romanov, N.G., Babunts, R.A., Shakhov, F.M., Kidalov, S.V., Vul', A.Y., Mamin, G.V., Orlinskii, S.B., and Silkin, N.I., Enormously high concentrations of fluorescent nitrogen-vacancy centers fabricated by sintering of detonation nanodiamonds, *Small*, 2011, vol. 7, no. 11, pp. 1533–1537. https://doi.org/10.1002/smll.201001887

11. Boudou, J.P., Curmi, P.A., Jelezko, F., Wrachtrup, J., Aubert, P., Sennour, M., Balasubramanian, G., Reuter, R., Thorel, A., and Gaffet, E., High yield fabrication of fluorescent nanodiamonds, *Nanotechnology*, 2009, vol. 20, no. 23, p. 235602. https://doi.org/10.1088/0957-4484/20/23/235602

12. Tisler, J., Balasubramanian, G., Naydenov, B., Kolesov, R., Grotz, B., Reuter, R., Boudou, J.-P., Curmi, P.A., Sennour, M., Thorel, A., Börsch, M., Aulenbacher, K., Erdmann, R., Hemmer, P.R., Jelezko, F., and Wrachtrup, J., Fluorescence and spin properties of defects in single digit nanodiamonds, *ACS Nano*, 2009, vol. 3, no. 7, pp. 1959–1965. https://doi.org/10.1021/nn9003617

13. Vaijayanthimala, V., Lee, D.K., Kim, S.V., Yen, A., Tsai, N., Ho, D., H.-Ch. Chang, and Shenderova, O., Nanodiamond-mediated drug delivery and imaging: Challenges and opportunities, *Expert Opin. Drug Delivery*, 2015, vol. 12, no. 5, pp. 735–749. https://doi.org/10.1517/17425247.2015.992412

14. Chao, J.I., Perevedentseva, E., Chung, P.H., Liu, K.K., Cheng, C.Y., Chang, C.C., and Cheng, C.L., Nanometer-sized diamond particle as a probe for biolabeling, *Biophys. J.*, 2007, vol. 93, no. 6, pp. 2199–2208. https://doi.org/10.1529/biophysj.107.108134

15. Pandey, K.C., New dimerized-chain model for the reconstruction of the diamond (111)-(2 1) surface, *Phys. Rev. B*, 1982, vol. 25, no. 6, pp. 4338–4346. https://doi.org/10.1103/PhysRevB.25.4338

16. Aleksenskii, A.E., Vul', A.Y., Konyakhin, S.V., Reich, K.V., Sharonova, L.V., and Eidel'man, E.D., Optical properties of detonation nanodiamond hydrosols, *Phys. Solid State*, 2012, vol. 54, pp. 578–585. https://doi.org/10.1134/S1063783412030031

17. Williams, O.A., Hees, J., Dieker, C., Jager, W., Kirste, L., and Nebel, C.E., Size-dependent reactivity of diamond nanoparticles, *ACS Nano*, 2010, vol. 4, no. 8, pp. 4824–4830. https://doi.org/10.1021/nn100748k

18. Vezo, O.S., Voitylov, A.V., Voitylov, V.V., et al., Aggregation of diamond and graphite particles in aqueous $AlCl_3$ electrolytes. Electrooptical studies, *Colloid J.*, 2022, vol. 84, pp. 243–253. https://doi.org/10.1134/S1061933X22030139

19. Petrov, M.P., Shilov, V.N., Trusov, A.A., Voitylov, A.V., and Vojtylov, V.V., Electro-optic research of polarizability dispersion in aqueous polydisperse suspensions of nanodiamonds, *Colloids Surf.*, A, 2016, vol. 506, pp. 40–49. https://doi.org/10.1016/j.colsurfa.2016.05.087

20. Popov, C., Kulisch, W., Gibson, P.N., Ceccone, G., and Jelinek, M., Growth and characterization of nanocrystalline diamond/amorphous carbon composite films prepared by MWCVD, *Diamond Relat. Mater.*, 2004, vol. 13, nos. 4–8, pp. 1371–1376. https://doi.org/10.1016/j.diamond.2003.11.040

21. Popov, C., Kulisch, W., Boycheva, S., Yamamoto, K., Ceccone, G., and Koga, Y., Structural investigation of nanocrystalline diamond/amorphous carbon composite films, *Diamond Relat. Mater.*, 2004, vol. 13, nos. 11–12, pp. 2071–2075. https://doi.org/10.1016/j.diamond.2004.04.001

22. Xu, H., Zang, J., Yuan, Y., Yan, S., Tian, P., Wang, Y., and Xu, X., Fabrication and microstructural characterization of the diamond@amorphous carbon nanocomposite core/shell structure via in-situ polymerization, *Ceram. Int.*, 2019, vol. 45, no. 15, pp. 18430–18438. https://doi.org/10.1016/j.ceramint.2019.06.060

23. Vul', A.Ya., Eydelman, E.D., Sharonova, L.V., Aleksenskiy, A.E., and Konyakin, S.V., Absorption and scattering of light in nanodiamond hydrosols, *Diamond Relat. Mater.*, 2011, vol. 20, no. 3, pp. 279–284. https://doi.org/10.1016/j.diamond.2011.01.004

24. Calderón-Martínez, M.C., Gil-Tolano, M.I., Navarro-Espinoza, S., Meléndrez, R., Chernov, V., and Barboza-Flores, M., Optical properties and functional groups characterization of commercial HPHT micro-diamond samples, *Opt. Mater.*, 2022, vol. 131, p. 112592. https://doi.org/10.1016/j.optmat.2022.112592

25. Vuks, M.F., *Elektricheskie i opticheskie svoistva molekul i kondensirovannykh sred* (Electrical and Optical Properties of Molecules in Condensed Matter), Leningrad: Leningr. Gos. Univ., 1984.

26. Graham, S.C., The refractive indices of isolated and of aggregated soot particles, *Combust. Sci. Technol.*, 1974, vol. 9, nos. 3–4, pp. 159–163. https://doi.org/10.1080/00102207408960351

27. Van de Hulst, H.C., *Light Scattering by Small Particles*, Dover Publications, 1981.

28. Born, M. and Wolf, E., *Principles of Optics: Electromagnetic Theory of Propagation, Interference and Diffraction of Light*, 1959.

29. Shifrin, K.S., *Rasseyanie sveta v mutnoi srede* (Light Scattering in Turbid Media), Moscow: Goslitizdat, 1951.

30. Trusov, A.A. and Vojtylov, V.V., *Electrooptics and Conductometry of Polydisperse Systems*, CRC Press, 1993.

31. Denisov, S.A., Dzidziguri, E.L., Spitsyn, B.V., Sokolina, G.A., and Boldyrev, N.Yu., Purification and modification of diamond detonation synthesis product,

Uch. Zap. Petrozavodsk. Gos. Univ., 2011, no. 2, pp. 89–98.

32. Klemeshev, S.A., Petrov, M.P., Rolich, V.I., Trusov, A.A., Voitylov, A.V., and Vojtylov, V.V., Static, dynamic and electric light scattering by aqueous colloids of diamond, *Diamond Relat. Mater.*, 2016, vol. 69, pp. 177–182. https://doi.org/10.1016/j.diamond.2016.08.016
33. Shifrin, K.S., Light scattering on double-layer particles, *Izv. Akad. Nauk SSSR, Ser. Geofiz.*, 1952, no. 2, pp. 15–21.
34. Iwaki, M., Estimation of the atomic density of amorphous carbon using ion implantation, SIMS, and RBS, *Surf. Coat. Technol.*, 2002, vol. 158, pp. 377–381. https://doi.org/10.1016/S0257-8972(02)00247-5

Translated by V. Kudrinskaya